Correlation of melting points of inositols with hydrogen bonding patterns

Alexandra Simperler,[a] Stephen W. Watt,[a] P. Arnaud Bonnet,[a] William Jones*[a] and W. D. Samuel Motherwell*[b]

Received 2nd May 2006, Accepted 22nd June 2006
First published as an Advance Article on the web 24th July 2006
DOI: 10.1039/b606107a

The melting points of seven inositol isomers cover a range of 180–350 °C although the only difference between them is the ratio of axially/equatorially orientated hydroxyl groups. All seven isomers feature infinite and finite hydrogen bond patterns and the type and occurrence of these patterns are explored as useful criteria for the prediction of melting points. All the patterns are classified into chain and ring motifs and atomistic and quantum chemical calculations are employed to evaluate the strength of interaction between pairs of molecules contributing to a pattern. There are four types of hydrogen bonded chains with three different types of molecular interactions—one strong and two weak ones. All high melting inositols (scyllo-, neo- and epi-inositol) possess infinite hydrogen bonded double chains with strong links and the number of chains per molecule correlates with their melting points. The lowest melting isomer (allo-inositol) shows no such double chains and only two single hydrogen bonded chains.

1. Introduction

In general terms, the melting point of a molecular crystal is correlated with its lattice energy, such that the higher the lattice energy of a crystal the higher will be the melting point. This generalisation, however, provides no indication of the main factors governing the melting process. Previous studies[1–8] have described a subtle and complex interplay of density, packing features, entropy, molecular structure, and strength and nature of the intermolecular interactions that will determine whether a molecular crystal melts at a relatively low or high temperature.

Ubbelohde[9] summarised in 1965 all available theories and approaches linking the process of melting and crystal structure. Several of the theories were, and remain, applicable to only the most simple systems. In the case of molecular crystals with complex interactions a simple correlation with structural features such as hydrogen bond geometry is not generally possible, but systematic studies of isomeric molecules may reveal some important factors.

The inositol[10] family of hexahydroxycyclohexanes (Scheme 1) provides an interesting example of how subtle variations in molecular structure markedly influence melting temperature (the inositols differ only in the distribution of axial or equatorial hydroxyl groups). All seven inositol isomers have twelve intermolecular O–H···O hydrogen bonds per molecule in their respective crystal lattices (see below), yet possess significant melting point differences from 180 to 350 °C (Table 1). The crystal densities correlate to some extent with the melting points, so the melting temperatures might be simply explained with the quality of packing; higher density generally implies higher melting point. However, there is a

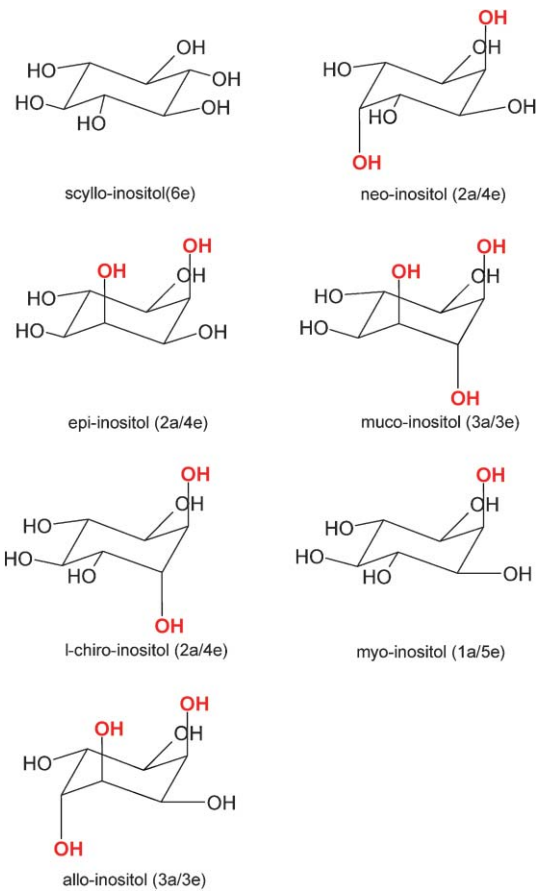

Scheme 1 Structure of inositol isomers.

[a]*The Pfizer Institute for Pharmaceutical Materials Science, Department of Chemistry, University of Cambridge, Lensfield Road, Cambridge, UK, CB2 1EW. E-mail: wj10@cam.ac.uk; Tel: +44 (0)1223-336468*
[b]*The Pfizer Institute for Pharmaceutical Materials Science, Cambridge Crystallographic Database Centre, 12 Union Road, Cambridge, UK, CB2 1EZ. E-mail: motherwell@ccdc.cam.ac.uk; Tel: +44 (0)1223-336021*

Table 1 Properties of the inositol crystals

Inositol isomer	T_m/C°	ρ/g cm^{-3}	Ratio ax/eq	Space group	Z	Z'^c	Number of hydrogen bonded neighbour molecules	CSD Ref. Code	Ref.
scyllo	350	1.58	0/6	$P\bar{1}$	2	1	8	—[a]	14
neo	315[b]	1.69	2/4	$P\bar{1}$	1	0.5	6	YEPNOW	18
epi	304[b]	1.66	2/4	$P2_1/c$	4	1	7	EPINOS	19
muco	290[b]	1.65	3/3	$P2_1$	4	1	11	MUINOS	20
L-chiro	246	1.60	2/4	$P2_1$	2	1	12	FOPKOK	21
myo	225[b]	1.58	1/5	$P2_1/c$	8	2	7	MYINOL	22
allo	180	1.68	3/3	$P2_1/n$	4	1	8	—[a]	15

[a] Recently determined unpublished structures, melting points determined by DSC. [b] Chapman and Hall, *Dictionary of Organic Compounds*, vol. 4, 6th edn (Electronic Publishing Division, 1996), otherwise T_m taken from ref. [c] Z' defines the number of molecules in the asymmetric unit; however, scyllo-inositol has two half molecules per asymmetric unit, giving two independent molecules.

severe anomaly in that allo-inositol has almost the highest density, but lowest melting point. Also scyllo-inositol having the equal-lowest density has the highest melting point.

Watt *et al.*[11] could successfully calculate the difference in melting points of neo- and myo-inositol using molecular dynamics but their method did not suggest a reasonable structural explanation. To gain some insight into the effect of possible hydrogen bonding patterns on melting points, we examined the various hydrogen bonding motifs existing within the available inositol crystals structures. Because hydroxyl groups are able to function simultaneously as a proton donor and acceptor, the inositols are able to build cooperative hydrogen bond networks, which were carefully examined and characterised.

During this analysis our attention was soon drawn to the prominent motif of an infinite ···O–H···O–H···O–H··· chain. As a result of such cooperative effects the hydrogen bonds in such chain motifs are particularly strong.[12] In several inositol structures, 'double chains' are formed as a result of particular inositol molecules involving two adjacent hydroxyl groups. Further, the occurrence of 'double chains' appeared to coincide satisfactorily with the melting temperatures—the more double chains per molecule in a crystal, the higher the melting point.

This phenomenological (and chemically oriented) approach based upon molecular properties fits quite well with the vibrational theories of melting: atomic or particle theories of matter describes melting as a process where thermal energy, dissipated in a crystal, causes some 'thermal motion' of the molecules around their sites in the crystal lattice. According to Lindemann,[9,13] if the molecules move too far from their equilibrium position, the crystal will become mechanically unstable. If the molecules, however, are part of a more extended structure, such as a chain or a stack, in which they are hydrogen bonded in a highly cooperative way, the whole chain or stack of molecules may adopt a frequency of vibration due to the thermal energy. There will also be a greater resistance for a molecule within such an extended arrangement to move from its initial equilibrium position as there are strong forces linking each molecule to several of its neighbours in the chains. A chain composed of strong links is less likely to break under thermal vibration than one composed of weak links.

We suggest that the melting points of the inositol crystals are dependent on two main factors: (i) how many cooperative hydrogen bonded motifs are present within the crystal and (ii) the "quality" of the individual links within these motifs (*i.e.* the intrinsic weakness/strength of a chain). In this paper, we identify and consider the hydrogen bond motifs occurring in the seven inositol crystal structures, describing them qualitatively. We then attempt to reveal in a quantitative manner their intrinsic weaknesses using quantum chemical methods to estimate the strength of the interaction between hydrogen bonded pairs of molecules.

2. Materials and methods

Inositols[10,14] are hexahydroxycyclohexanes and exist as seven optically inactive meso-forms and one optically active D,L-pair. Each isomer only differs from each other in the equatorial or axial position of the six hydroxyl-groups—see Scheme 1 (axial groups shown in red).

The crystal structures of neo-, epi-, muco-, L-chiro and myo-inositol have been taken from the Cambridge Structural Database (CSD);[15,16] CSD reference codes are shown in Table 1. The crystal structures of scyllo- and allo-inositol are taken from recent unpublished work[17,18] from our laboratory.

Table 1 comprises a survey on the most relevant data of the inositol crystals whilst Fig. 1a to 1i show the individual inositol molecules where all axial hydroxyl groups are highlighted. The conformation of the molecules, and in particular the orientation of the hydroxyl groups, are as found in the crystal structures. Intermolecular O–H···O hydrogen bond distances are also shown (calculated using Materials Studio[19]). The following criteria were used: a maximum hydrogen–acceptor distance of 2.5 Å and a minimum donor–hydrogen–acceptor angle of 90°.

The starting geometries of molecules for the energy study of hydrogen-bonded pairs were obtained from supercells of the respective inositol containing 128 molecules. The lattice parameters of the supercells as well as all geometry parameters of all molecules in the supercells were geometry optimised using the DISCOVER code[19] with the COMPASS[20] force field.

The quantum chemical calculations were performed with the DMol^3 program,[21] employing a PW91[22] density functional and the dnp basis set (*i.e.*, a double numerical basis function with polarization functions). DMol^3 does not have a basis set superposition error (BSSE) option, as BSSE in DFT calculation is considered to be small[23] and a numerical basis set is used.

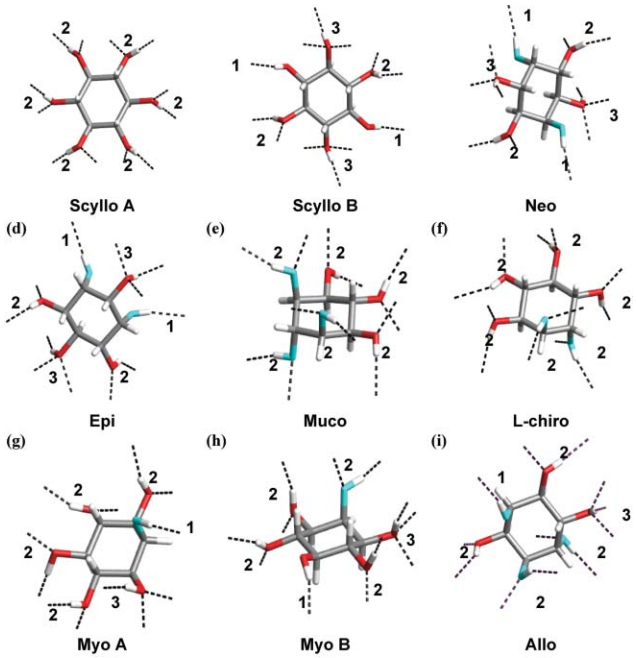

Fig. 1 Inositol isomers with hydrogen bonds (see text for definition). The axial OH groups are highlighted in turquoise. The numbers of hydrogens bond per OH group are shown beside each group.

Free hydroxyl groups within the molecular isolated pairs/dimers (*i.e.* those not involved in pair formation) in the gas phase were arranged manually to form intramolecular hydrogen bonds. In contrast to the situation in the condensed phase, the hydroxyl groups for the molecules in the gas-phase are expected to orientate in a way to maximise the number of internal hydrogen bonds.[24,25]

Each molecular pair was allowed to relax without imposing any constraint on any geometrical parameter of the pairs during DFT energy optimisation. The strength of the intermolecular bond was observed to be sufficient to maintain the nature of the pair interaction so implementing constraints upon the dimer was not necessary. The interaction energy, E_{int}, was calculated as:

$$E_{int} = E_{dimer} - 2E_{monomer} \quad (1)$$

where E_{dimer} is the energy of a gas phase dimer, and $E_{monomer}$ is the energy of a gas phase monomer.

3. Results and discussion

3.1. Relationship between melting point and structural features

The packing arrangement of molecules in a molecular crystal is governed by the interplay of the tendency to close packing and the strength of intermolecular interactions. We expect the lattice energy in the particular case of inositols to be dominated by strong O–H···O bonds. The sum of non-bonded van der Waals interactions will be strongest for the most dense structure; thus, one would expect inositol isomers with a high density and a large number of hydrogen bonds between the molecules to be particularly stable, and have a high melting point. However, we note in Table 1 that scyllo-inositol is anomalous having the lowest density but the highest melting point.[17] Further, we see that allo-inositol has the second highest density but the lowest melting point.

We note that in all inositol crystals the molecules have twelve intermolecular hydrogen bonds to nearest neighbours so the simple criterion of counting hydrogen bonds does not explain melting point differences. However, the pattern of hydrogen bonding varies considerably. Previous research[12,26–30] has shown that the strength of infinite chain hydrogen bonds is not the sum of the corresponding isolated intermolecular interactions, rather, the total energy of these hydrogen bond configurations will be lower due to cooperative effects. In hydrogen patterns such as ···O–H···O–H···O–H··· the cooperative effect is referred to as σ-cooperativity.[27] The intermolecular hydrogen bond strength per link increases in a nonlinear fashion as a function of the number of molecules in these chains or pattern until it converges to the asymptotic value for the infinite chain.[31]

In the following section, the particular hydrogen bond patterns occurring in each of the crystals of the inositol isomers will be examined in an attempt to relate the types and frequency of hydrogen bond patterns to low or high melting temperatures.

3.2. Relation between melting points and hydrogen bonding patterns

The inositol molecules and associated hydrogen bond connections are shown in Fig. 1 together with the number of hydrogen bonds per OH group. It is observed that hydroxyl groups are associated with either one, two or three hydrogen bonds. If an OH group is involved in one hydrogen bond it always acts as a proton donor and this feature is predominantly found for axial hydroxyl groups as shown previously in a general survey of axial and equatorial OH groups.[32] No instances are observed where a hydroxyl group is an acceptor without also acting as a donor. The single hydrogen bonded OH groups naturally act as chain terminators, or form discrete hydrogen bonds as opposed to cooperative chains. Most of the OH groups are found to act as both donors and acceptors making them potential contributors to hydrogen bond chains, and both axial and equatorial OH groups participate in such chains. Finally, we observe that only the equatorial OH groups participate in three hydrogen bonds, where the OH group donates a proton and accepts simultaneously two protons. These OH groups contribute to a chain and also to a discrete hydrogen bond.

Chains and sheets. We examine first neo-inositol (Fig. 2) because it has an easily visualised hydrogen bonded network and is thus ideal to discuss the difference between chains and discrete hydrogen bonds. The two blue arrows in Fig. 2a indicate an infinite chain and the molecules participating in this chain are shown highlighted in colour. Fig. 2b shows the H-bond chain in isolation.

The complete 3-D structure can be visualised as stacks of sheets linked by these infinite chains. The blue dotted line in Fig. 2a marks the position of a sheet in neo-inositol with respect to the direction of the stacks. Fig. 2c shows how the

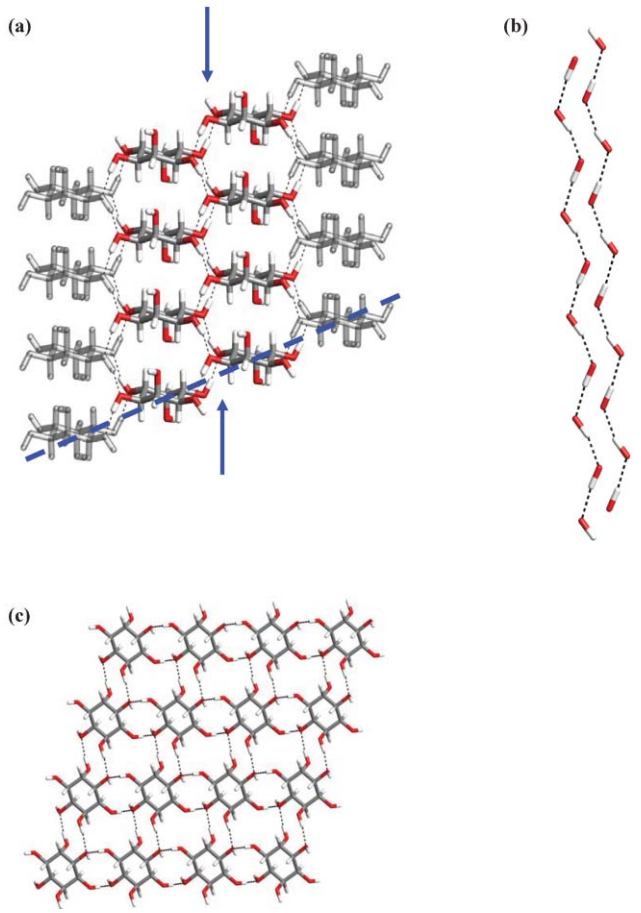

Fig. 2 Neo-inositol (a) stacks, (b) isolated hydrogen bond chain, (c) sheet of molecules with discrete hydrogen bonds. The blue arrows show the direction of the hydrogen bond chain and the blue dashed line shows the plane of a sheet of molecules.

discrete hydrogen bonds link molecules in the plane of the sheet. All the other inositols may be visualised as being similarly 'constructed'—with stacks and sheets—except muco- and L-chiro-inositol, both of which comprise sheets without any evidence of stacks. Muco-inositol is the only inositol with a ring rather than an infinite chain motif, and L-chiro-inositol displays meandering single chains, which do not allow a conceptually 'neat' stacking of molecules.

Cooperative chains. In Fig. 3, all cooperative hydrogen bonding patterns occurring in the seven inositol crystals are presented showing only those OH groups involved. The black dashed lines indicate the hydrogen bonds forming infinite chains, whereas blue dashed lines indicate additional hydrogen bonds between these chain linked molecules. The latter do not contribute to the cooperative chain but contribute indirectly to the strength of a hydrogen bond chain by providing an additional link between two adjacent molecules.

With scyllo-inositol, pairs of molecules and single molecules are contributing in turn with two and one OH groups, respectively, to a double chain (Fig. 3a). Also, the single molecules have an additional non-cooperative hydrogen bond linking the stacked molecules. Each scyllo-inositol molecule A (Fig. 1a) takes part in three double chains, whereas a scyllo-inositol molecule B (Fig. 1b) contributes only to two double chains.

Neo-inositol shows a very simple double chain as can be clearly seen in Fig. 3b. Each molecule participates in two double chains with two adjacent OH groups at a time.

Epi-inositol has the same pattern of double chains (Fig. 3c) as neo-inositol, and further, comprises single chains, as shown in Fig. 3d. In these single chains two consecutive molecules are linked *via* two hydrogen bonds but only one of these hydrogen bonds contributes to the single chain.

Muco-inositol is the only inositol isomer which has ring motifs (Fig. 3e) instead of chains. Ten molecules participate using twelve OH groups to form these ring motifs, with every OH involved in two hydrogen bonds. Two out of the ten muco-inositol molecules are participating with two adjacent OH groups. Each molecule participates in five such ring motifs: one motif with two adjacent OH groups and another four motifs with one hydroxyl group at a time.

L-chiro-inositol (Fig. 3f) shows that every OH group is involved with two hydrogen bonds and participates in a single chain. Each molecule participates in six single chains which meander in a quite unstructured manner throughout the crystal, forming a complex hydrogen bond pattern.

Myo-inositol has a similar double chain to scyllo-inositol, which is apparent when Fig. 3a and Fig. 3g are compared. Again, pairs of molecules contributing two OH groups to the double chain and a single molecule contributing a single OH group are alternating. The inserted single molecule is on one hand linking the double bonded units by contributing one OH group to the chain and on the other hand with two non-cooperative hydrogen bonds (see blue dashed lines in Fig. 3g). The crucial difference between myo- and scyllo-inositol is that in the myo-inositol crystal only two of these double chains are present per molecule whereas in scyllo-inositol there are three. Additionally, it is noted that the direction of hydrogen bonding in the two strands is different. This will be discussed further below.

Allo-inositol has a cooperative hydrogen bond pattern which can be described as a single chain with loops (Fig. 3h). In Fig. 3i, the three allo-inositol molecules which donate one OH into the loop-motif are omitted for clarity. A cooperative loop-motif commences with an axial OH group, which serves only as proton donor (marked with 1 in Fig. 1i and indicated with a blue arrow in Fig. 3i, respectively), and is finished with an equatorial OH group that simultaneously propagates the chain (marked 3 in Fig. 1i and indicated with a green arrow in Fig. 3i, respectively). Thus, every allo-inositol molecule participates in two chain and four loop motifs in the crystal.

3.3. Categories of chains

We classify the chains into four categories according to the direction of hydrogen bonding (see Fig. 4a–d):

Type I regular double chain – antiparallel
Type II irregular double chain – antiparallel
Type III irregular double chain – parallel
Type IV single chain

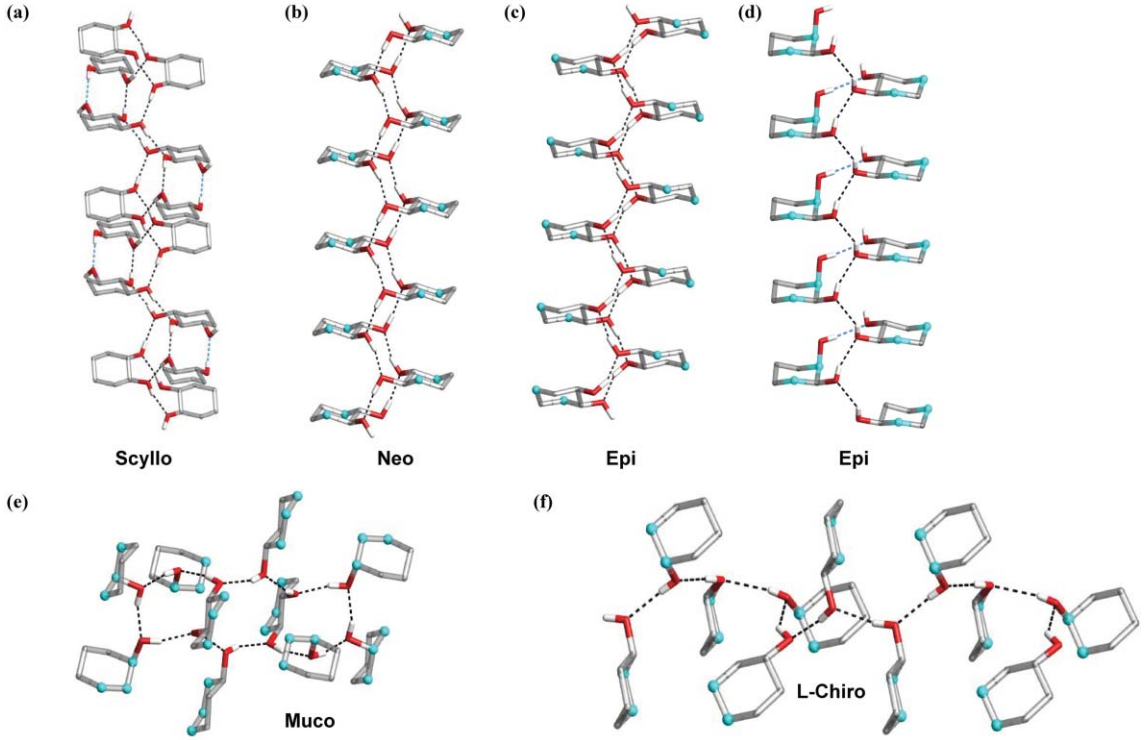

Fig. 3 Cooperative hydrogen bond patterns shown as black dashed lines. Only the OH groups involved in cooperative patterns are shown. Carbons with axial OH groups are shown in turquoise.

Double chains are created when some or all of the inositol molecules contribute with two adjacent OH groups to a chain motif as opposed to single chains where only one OH group is involved. The green arrows in Fig. 4 point along the hydrogen bond direction. In chain types I and II the arrows indicate that the hydrogen bonds are oriented antiparallel (Fig. 4a and 4b), whereas they are parallel in the chain of type III (Fig. 4c). The chains can be *regular*, meaning that each inositol molecule contributes with two adjacent OH groups to the double chain (type I), or *irregular*, as in the chains of type II and III, where

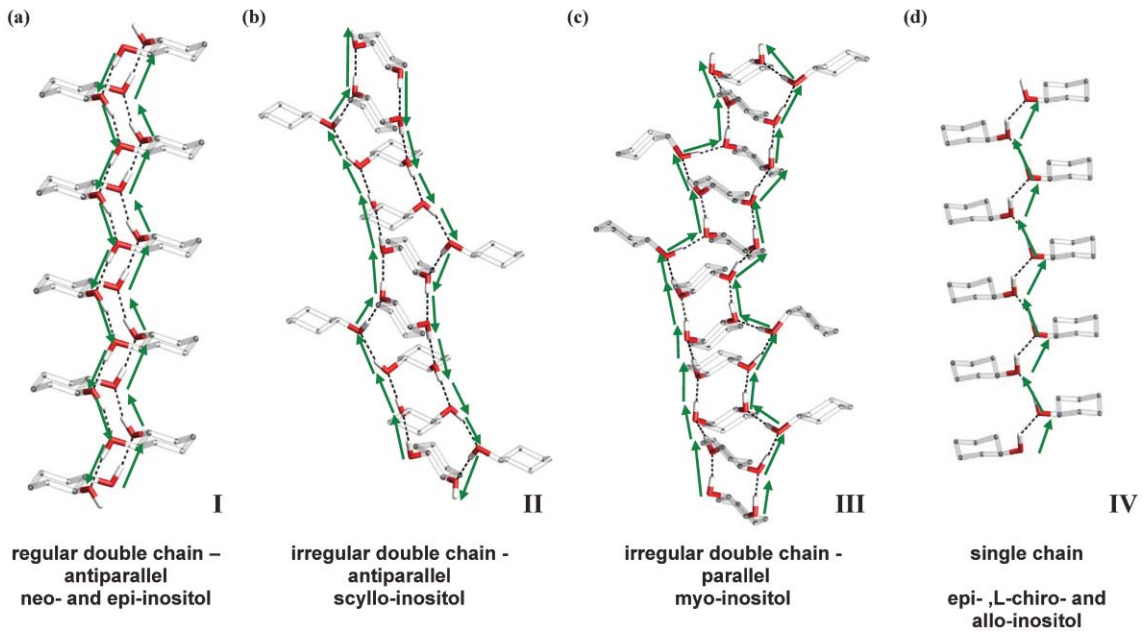

Fig. 4 Types of infinite hydrogen bond chains. (a) Type I, (b) type II, (c) type III and (d) type IV. The green arrows indicate the direction of the individual hydrogen bonds, *i.e.* → indicates O–H···O.

molecules contributing two OH groups are alternating with a molecule contributing only one.

Scyllo-inositol has two independent molecules in the asymmetric unit cell which we refer to as scyllo A and scyllo B. Each scyllo-inositol molecule contributes to three (scyllo A) or two double chains (scyllo B) of type II, a neo-inositol molecule to two double chains of type I, whereas an epi-inositol molecule contributes to one of type I and two single chains (type IV). Muco-inositol does not have chains but five ring motifs per molecule, and in the L-chiro-inositol crystal, the six hydroxyl groups of a molecule contribute to six different chains of type IV. Myo-inositol molecules are involved in the formation of two double chains of type III. In allo-inositol, the lowest melting in the inositol family, each molecule contributes to two chains of type IV and four loop motifs (Fig. 3i).

Summary of counts of double chains. It is noteworthy that the three highest melting inositols have double chains in the crystal and the numbers per molecule (3 and 2, 2, and 1 for scyllo-, neo-, and epi-inositol, respectively) coincide perfectly with the order of melting temperature. The five ring motifs in muco-inositol provide a reasonable cooperativity effect within the contributing twelve OH groups, which may explain the melting point for this crystal lying below those of the inositols with double chains and above those of L-chiro- and allo-inositol with six and two single chains. The unusual isomer is myo-inositol; with two double chains—it might be expected to have a much higher melting point. Thus, the presence of double chains alone does not guarantee a high melting point—we consider the strengths of the links in the next section.

3.4. Relation between melting points and quality of hydrogen bond chains

The 'weakest link' of a chain is essentially a weak interaction between two individual molecules. The strength of any link can be increased by cooperative effects, but we can envisage that as the crystal is heated and thermal vibration amplitudes increase, the weakest link will be the first to break. We now identify and quantify all the observed molecule–molecule interactions in the inositol crystals. To cover the whole range of occurring molecule–molecule interactions it is sufficient to pick one reference molecule and all of its n hydrogen bonded neighbours (n = 6, 7, 11, 12, and 8 for neo-, epi-, muco-, L-chiro- and allo-inositol, respectively—see Table 1). In the cases of scyllo- and myo-inositol, where there are two molecules in the asymmetric unit cell, both the molecules and their hydrogen bonded neighbours have to be considered (n = 8 and 7 for scyllo- and myo-inositol, respectively). We now consider the energy of the interaction with each neighbour by examining the isolated pairs of molecules, *i.e.* dimers.

Energy of free molecules. The gas phase dimers were selected and their energy (E_{dimer}) calculated as described in section 2.2. To establish the interaction energy, E_{int}, it was necessary to calculate energies for the seven inositol monomers as isolated molecules. The order of the inositol monomers with respect to decreasing stability is as follows: neo > epi > myo > allo > scyllo > muco > L-chiro (Fig. 5a–g). Not surprisingly, there is no correlation with the observed melting point of the corresponding crystals. A crucial factor governing the stability of a monomer is the number of intramolecular hydrogen bonds (denoted with black lines in Fig. 5); such

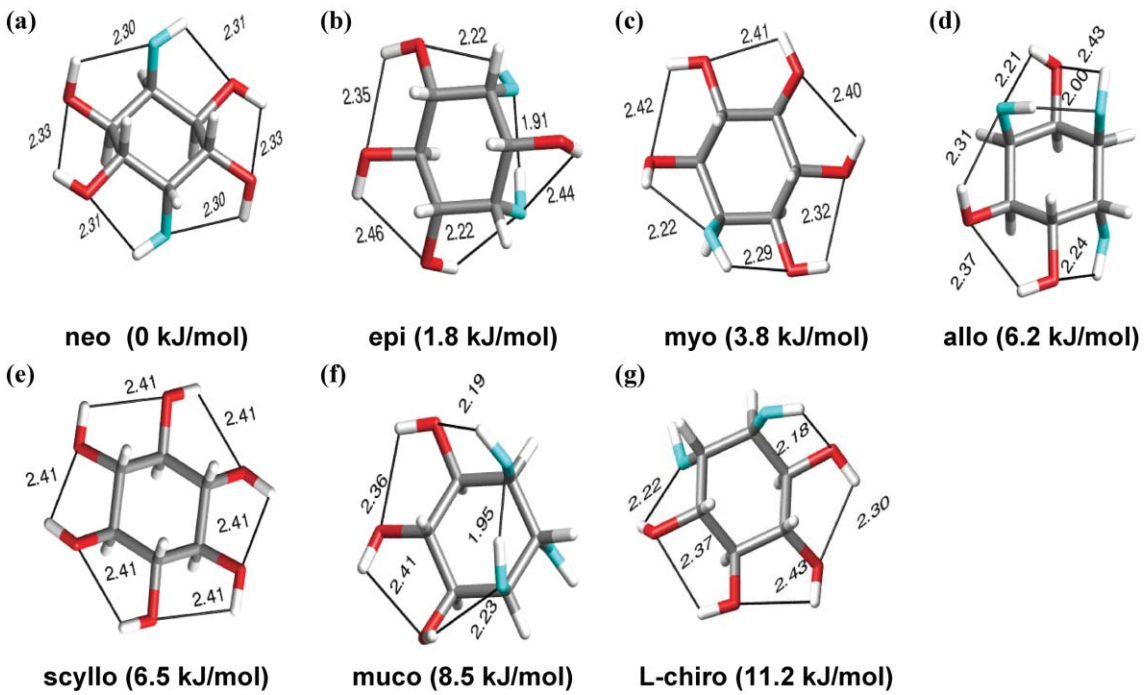

Fig. 5 Relative energies in the gas phase of inositol molecules after full minimisation. The energy is relative to the lowest of the set, neo-inositol. Intramolecular hydrogen bond distances are shown [Å].

intramolecular interactions are not present in the crystal. Thus, we cannot expect a direct relationship between stability of a monomer in the gas phase and the stability of the corresponding crystal.

Muco- and L-chiro-inositol (Fig. 5f and 5g), which are found to be the least stable monomers, have five intramolecular hydrogen bonds whereas the other five monomers have six. Muco- and L-chiro have axial OH groups adjacent to each other on the cyclohexane ring, and this severely disturbs the intramolecular hydrogen bond pattern. Scyllo-inositol (Fig. 5e), with all equatorial OH groups, occupies a position in the middle of the energy range. We notice that the presence of some axial OH groups, especially on opposite ends of the cyclohexane ring, is necessary to allow optimal intermolecular hydrogen bonding, as in neo-inositol (Fig. 5a). An axial OH in position 1,3 enables strong intramolecular hydrogen bonds to be formed, as in epi- and allo-inositol (Fig. 5b and 5d).

Energy of dimer formation in the gas phase. When two inositol monomers form a dimer, the intramolecular hydrogen bonds have to be broken and replaced by intermolecular bonds. Consequently, the interaction energy will be comprised of the energy needed to open the intramolecular bonds, the energy gained/lost by forming the dimer and the energy gained/lost, when the OH groups not involved in the intermolecular bond rearrange to form the maximum number of intramolecular hydrogen bonds.

If the interaction energy is negative it indicates that energy was gained (*strong* dimer), whereas a positive interaction energy shows that energy was needed to form the dimer (*weak* dimer). Weak dimers can be stabilised in the crystal due to the interactions with the neighbouring molecules; in particular by intermolecular hydrogen bonding. However, as molecules begin to move in larger amplitudes as temperature increases, we might expect the weak dimers to break more easily than the strong ones, since the interaction with the neighbours will be also weaker due to thermal motion. We might expect that weak dimers forming a link in a chain, indeed form a weak link, and consequently a lower melting point for the total crystal.

There are three types of interactions observed in the dimers (Fig. 6):

Type A a double hydrogen bond – antiparallel
Type B a double hydrogen bond – parallel
Type C a single hydrogen bond

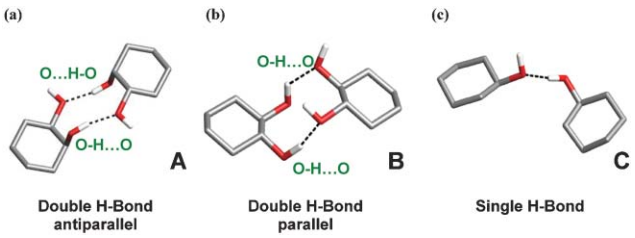

Fig. 6 Types of hydrogen bonds between pairs of inositol molecules. (a) Type A, (b) type B and (c) type C.

Anti-parallel and parallel refer to the direction of the cooperative hydrogen bonds as discussed above (Fig. 4). The results of the quantum chemical calculations of the pairs are given in Table 2. The first column comprises the specification of the molecule pairs: R refers to a reference molecule in the crystal and N_{1-12} indicate the molecules to which R is hydrogen bonded. The second column displays the interaction energies and the third column the type of interaction (*i.e.* A, B or C, see Fig. 6). Further, Table 2 gives information on the orientation of the interacting hydroxyl groups (*i.e. ax* and *eq* for axial or equatorial), details of the hydrogen bonding geometry (*i.e.* hydrogen bond distances and angles) and information on how much distortion is imposed on the cyclohexane rings of the monomers when forming a dimer. The torsion angle $t(\text{O–C–C–O})_{\text{mono}}$ is the torsion in the monomer in the gas phase whereas t(O–C–C–O) is the torsion when the monomer is interacting with another monomer. The difference of these two values, Δt(O–C–C–O), may serve as rough guide on how intermolecular hydrogen bonds change the strain within the O–C–C–O moiety of the cyclohexane ring participating in intermolecular hydrogen bonding.

From the quantum chemical calculations on the dimers we conclude the important fact that in general all dimers of type A can be expected to be stable in the gas phase whilst all dimers of type B and C result in unfavourable interaction energies. However, we note that for two dimers of type A for allo-inositol there are positive interaction energies: the intramolecular hydrogen bonding arrangement of an allo-inositol monomer (Fig. 5d) becomes severely interrupted when a dimer is formed, and the intermolecular hydrogen bonds cannot compensate for loss of this intramolecular energy.

Examination of the axial and equatorial nature of participating OH groups, shows no recognisable correlation with interaction strength, *i.e.* no axial/equatorial combination is particularly favoured in energy.

The hydrogen bond distances, d(O–H···O), range from 1.74–1.92 Å for dimers type A, 1.74–2.30 Å for dimers type B and 1.76–1.94 Å for dimers type C, respectively. The hydrogen bond angles, a(O–H···O), cover a range from 130 to 178°. Generally, the strength or weakness of a hydrogen bond can be estimated by its geometry – *i.e.* the shorter the hydrogen bond distance and the closer the hydrogen bond angle to 180° the stronger is the hydrogen bond.[12] A plot of the hydrogen bond distances *vs.* angles (Fig. 7) for the double hydrogen bonded dimers shows that the geometry of dimers type A indicate strong hydrogen bonds whilst the data of type B suggest weaker hydrogen bonds. This result is in agreement with the calculated interaction energies, E_{int}. A peculiarity occurs with all dimers of type B where one of the hydrogen bonds is much longer than the other one, *i.e.* 2.14 to 2.29 Å compared to 1.73 to 1.99 Å. Also, one of the hydrogen bond angles is less obtuse—one ranges from 130 to 136° whereas the other one from 160 to 166°. The dimer attempts to avoid the unfavourable interaction by breaking one hydrogen bond. Only an accurate initial arrangement of the intermolecularly bound OH groups prevents the dimer from breaking during minimisation—the dimer is only just at a state where both the hydrogen bonds are still intact. A similar phenomenon can be noted with the two unfavourable type A dimers of

Table 2 Interaction energies, E_{int}, between the individual dimers, description of the hydrogen bond type, description of the position of the OH group comprising acceptor or donor atoms for the reference molecule R and its neighbours N_{1-12}, as defined in text, intermolecular hydrogen bond distances, d(O···H), hydrogen bond angles, a(O–H···O), and dihedral angles of the monomer inositol monomers, t(O–C–C–O)$_{mono}$, and within the hydrogen bonds of the dimers, t(O–C–C–O), and the relative difference between dimer and monomer, Δt(O–C–C–O)|

Inositol–dimer	E_{int}/kJ mol^{-1}	H-bond type	Position of donor/acceptor in molecule R	Position of donor/acceptor in molecules N_{1-12}	d(O···H)/Å	a(O–H···O)/°	t(O–C–C–O)$_{mono}$/°	t(O–C–C–O)/°	Δt|(O–C–C–O)|/°
scyllo A									
R_A-N_1	−5.7	A	**H_{eq}, O_{eq}**	O_{eq}, H_{eq}	1.809/1.809	162.7/162.7	−62.3/62.3	−62.7/62.7	0.4/0.4
R_A-N_2	19.5	C	**H_{eq}**	O_{eq}	1.832	166.4	—	—	—
R_A-N_3	−6.4	A	**H_{eq}, O_{eq}**	O_{eq}, H_{eq}	1.794/1.794	167.3/167.3	−62.3/62.3	−64.6/64.6	2.3/2.3
R_A-N_4	11.3	C	**O_{eq}**	H_{eq}	1.847	171.0	—	—	—
R_A-N_5	−5.7	A	**H_{eq}, O_{eq}**	O_{eq}, H_{eq}	1.809/1.809	162.7/162.7	−62.3/62.3	−62.7/62.7	0.4/0.4
R_A-N_6	19.5	C	**H_{eq}**	O_{eq}	1.832	166.4	—	—	—
R_A-N_7	−6.4	A	**H_{eq}, O_{eq}**	O_{eq}, H_{eq}	1.794/1.794	167.3/167.3	−62.3/62.3	−64.6/64.6	2.3/2.3
R_A-N_8	11.3	C	**O_{eq}**	H_{eq}	1.847	171.0	—	—	—
scyllo B									
R_B-N_1	−6.3	A	O_{eq}, H_{eq}	**H_{eq}, O_{eq}**	1.784/1.784	166.1/166.1	−62.3/−62.3	−64.7/64.7	2.4/2.4
R_B-N_2	14.8	C	O_{eq}	**H_{eq}**	1.836	162.3	—	—	—
R_B-N_3	−6.3	A	O_{eq}, H_{eq}	**H_{eq}, O_{eq}**	1.788/1.788	167.4/167.4	−62.3/−62.3	−64.4/64.4	2.1/2.1
R_B-N_4	11.4	C	H_{eq}	**O_{eq}**	1.845	170.8	—	—	—
R_B-N_5	−6.3	A	O_{eq}, H_{eq}	**H_{eq}, O_{eq}**	1.784/1.784	166.1/166.1	−62.3/−62.3	−64.7/64.7	2.4/2.4
R_B-N_6	14.8	C	O_{eq}	**H_{eq}**	1.836	162.3	—	—	—
R_B-N_7	−6.3	A	O_{eq}, H_{eq}	**H_{eq}, O_{eq}**	1.788/1.788	167.4/167.4	−62.3/−62.3	−64.4/64.4	2.1/2.1
R_B-N_8	11.4	C	H_{eq}	**O_{eq}**	1.845	170.8	—	—	—
Neo									
R-N_1	−10.8	A	H_{ax}, O_{eq}	O_{eq}, H_{ax}	1.788/1.772	169.0/168.7	−56.7/56.7	−61.5/61.8	4.8/5.1
R-N_2	−1.1	A	H_{eq}, O_{eq}	O_{eq}, H_{eq}	1.777/1.785	163.3/164.8	−59.9/59.9	−73.2/72.8	13.3/12.9
R-N_3	−1.0	A	H_{eq}, O_{eq}	O_{eq}, H_{eq}	1.782/1.805	162.3/162.5	−59.9/59.9	−71.2/71.0	11.3/11.1
R-N_4	−10.8	A	H_{ax}, O_{eq}	O_{eq}, H_{ax}	1.788/1.772	169.0/168.7	−56.7/56.7	−61.5/61.8	4.8/5.1
R-N_5	−1.1	A	H_{eq}, O_{eq}	O_{eq}, H_{eq}	1.777/1.785	163.3/164.8	−59.9/59.9	−73.2/72.8	13.3/12.9
R-N_6	−1.0	A	H_{eq}, O_{eq}	O_{eq}, H_{eq}	1.782/1.805	162.3/162.5	−59.9/59.9	−71.2/71.0	11.3/11.1
epi									
R-N_1	−1.8	A	H_{ax}, O_{eq}	O_{eq}, H_{ax}	1.793/1.817	170.4/169.3	−57.6/61.7	−60.6/60.7	3.0/1.0
R-N_2	8.1	B	H_q, H_{eq}	O_{eq}, O_{eq}	2.285/1.737	132.6/159.5	61.7/62.4	56.8/68.8	4.9/6.4
R-N_3	18.9	C	O_{eq}	H_{eq}	1.798	166.3	—	—	—
R-N_4	18.7	C	H_{eq}	O_{eq}	1.784	168.8	—	—	—
R-N_5	4.3	B	O_{eq}, O_{eq}	H_{eq}, H_{ax}	2.230/1.938	136.0/140.6	−66.5/−63.4	−64.4/−57.6	3.1/6.8
R-N_6	−3.4	A	H_{eq}, O_{eq}	O_{eq}, H_{eq}	1.774/1.771	160.2/160.0	62.4/−63.4	70.3/−70.2	7.9/6.8
R-N_7	−8.9	A	O_{eq}, H_{eq}	H_{eq}, O_{eq}	1.752/1.753	170.6/170.7	62.4/−63.4	67.3/−67.3	4.9/3.9
muco									
R-N_1	8.2	C	O_{eq}	H_{eq}	1.832	149.1	—	—	—
R-N_2	8.2	C	H_{eq}	O_{eq}	1.840	148.7	—	—	—
R-N_3	14.8	C	H_{ax}	O_{ax}	1.855	175.4	—	—	—
R-N_4	16.6	C	O_{ax}	H_{ax}	1.905	158.7	—	—	—
R-N_5	12.4	C	H_{eq}	O_{ax}	1.781	172.6	—	—	—
R-N_6	35.1	C	O_{eq}	H_{ax}	1.873	166.2	—	—	—
R-N_7	−3.3	A	H_{eq}, O_{eq}	O_{eq}, H_{eq}	1.826/1.821	155.3/154.9	−60.8/−60.8	−69.1/−69.2	8.3/8.4
R-N_8	14.6	C	H_{ax}	O_{ax}	1.845	174.8	—	—	—
R-N_9	16.3	C	O_{ax}	H_{ax}	1.893	158.8	—	—	—
R-N_{10}	28.8	C	H_{ax}	O_{eq}	1.780	167.6	—	—	—
R-N_{11}	13.1	C	O_{ax}	H_{eq}	1.758	174.3	—	—	—
L-chiro									
R-N_1	4.7	C	O_{ax}	H_{eq}	1.902	149.0	—	—	—
R-N_2	12.4	C	H_{ax}	O_{eq}	1.764	176.7	—	—	—
R-N_3	14.1	C	H_{ax}	O_{eq}	1.887	172.0	—	—	—
R-N_4	17.3	C	O_{eq}	H_{eq}	1.807	167.1	—	—	—
R-N_5	16.6	C	H_{eq}	O_{eq}	1.826	163.4	—	—	—
R-N_6	4.0	C	H_{eq}	O_{eq}	1.942	146.9	—	—	—
R-N_7	17.3	C	H_{eq}	O_{ax}	1.807	167.1	—	—	—
R-N_8	16.6	C	O_{eq}	H_{ax}	1.826	163.4	—	—	—
R-N_9	12.4	C	O_{eq}	H_{eq}	1.764	176.7	—	—	—
R-N_{10}	14.1	C	O_{eq}	H_{ax}	1.887	172.0	—	—	—
R-N_{11}	2.9	C	O_{ax}	H_{eq}	1.757	162.4	—	—	—
R-N_{12}	2.9	C	H_{eq}	O_{ax}	1.757	162.4	—	—	—
myo A									
R_A-N_1	−7.7	A	H_{ax}, O_{eq}	O_{eq}, H_{ax}	1.769/1.769	166.3/166.3	55.5/55.5	60.0/60.0	4.5/4.5
R_A-N_2	17.1	C	H_{eq}	O_{eq}	1.870	167.9	—	—	—
R_A-N_3	13.3	B	O_{eq}, O_{eq}	H_{eq}, H_{eq}	2.236/1.919	132.4/164.5	−60.9/62.3	−63.7/57.6	2.8/4.7
R_A-N_4	1.2	A	H_{eq}, O_{eq}	O_{ax}, H_{eq}	1.804/1.906	162.5/158.4	−54.1/62.0	−57.9/63.4	3.8/1.4
R_A-N_5	−9.6	A	H_{eq}, O_{eq}	O_{eq}, H_{eq}	1.774/1.766	170.3/169.7	−61.2/61.2	−63.1/62.9	1.9/1.7
R_A-N_6	13.2	B	H_{eq}, H_{eq}	O_{eq}, O_{eq}	1.923/2.279	166.3/130.3	−60.9/62.3	−63.9/58.1	3.0/4.2
R_A-N_7	9.4	C	O_{eq}	H_{eq}	1.778	168.4	—	—	—

Table 2 (*Continued*)

myoB									
R_B-N_1	1.1	A	O_{ax}, H_{eq}	H_{eq}, O_{eq}	1.820/1.904	162.6/157.5	−61.2/55.5	−62.9/58.1	1.7/2.6
R_B-N_2	−8.2	A	H_{ax}, O_{eq}	O_{eq}, H_{eq}	1.741/1.781	166.7/171.9	−54.1/62.0	−61.3/63.3	7.2/1.3
R_B-N_3	15.2	B	H_{eq}, H_{eq}	O_{eq}, O_{eq}	2.137/1.924	134.8/162.7	−60.9/62.3	−60.7/63.8	0.2/1.5
R_B-N_4	19.3	C	O_{eq}	H_{eq}	1.839	174.7	—	—	—
R_B-N_5	−8.0	A	O_{eq}, H_{eq}	H_{ax}, O_{eq}	1.739/1.780	166.4/172.1	62.0/55.5	62.8/61.0	0.8/5.5
R_B-N_6	11.7	C	H_{eq}	O_{eq}	1.806	165.5	—	—	—
R_B-N_7	13.2	B	O_{eq}, O_{eq}	H_{eq}, H_{eq}	1.986/2.149	160.5/132.4	62.3/62.3	61.5/60.1	0.8/1.2
allo									
R-N_1	−0.4	A	H_{ax}, O_{eq}	O_{eq}, H_{ax}	1.749/1.747	167.5/167.9	54.0/54.0	61.8/61.6	7.8/7.6
R-N_2	10.4	A	H_{eq}, O_{eq}	O_{ax}, H_{eq}	1.802/1.916	166.6/147.3	61.3/55.6	72.3/61.0	11.0/4.4
R-N_3	13.6	C	H_{eq}	O_{eq}	1.797	163.6	—	—	—
R-N_4	−1.5	A	O_{eq}, H_{ax}	H_{ax}, O_{eq}	1.760/1.760	173.5/173.5	55.9/55.9	63.7/63.7	7.8/7.8
R-N_5	14.2	C	O_{ax}	H_{eq}	1.849	169.8	—	—	—
R-N_6	10.4	A	O_{ax}, H_{eq}	H_{eq}, O_{eq}	1.802/1.916	166.6/147.3	61.3/55.6	72.3/61.0	11.0/4.4
R-N_7	13.6	C	H_{ax}	O_{ax}	1.797	163.6	—	—	—
R-N_8	14.2	C	O_{eq}	H_{eq}	1.849	169.8	—	—	—

allo-inositol (both +10.4 kJ mol^{-1}). The bond lengths are similar in order of magnitude whilst one of the hydrogen bond angles is more obtuse than the other one (167° as opposed to 147°).

Dimers of type C have only one hydrogen bond and as a consequence do not impose any severe strain on the cyclohexane ring. For type A and B, the two bonds are formed by two adjacent hydroxyl groups, and some strain can be expected. The dimers type B are less strained due to the fact that one of the hydrogen bonds is very long. The strain is notable only in dimers of type A where the two hydrogen bonds are equally strong. Most of the type A dimers have a Δt|(O–C–C–O)| value below 5° which corresponds to only a little strain. Some dimers of type A in neo-inositol and allo-inositol show values up to 13.3°, which usually go together with low but still favourable interaction energies.

In summary, we conclude that dimers of type A can be considered as strong links in hydrogen bond chains, whereas type B and C dimers are weak links and will be less resistant to thermal motion. Calculations performed with PLUTO [33] using the Gavezzotti empirical force field[34,35] on the actual dimers in the crystals show in links A and B interaction energies E_{int} from −10 to −13 kcal mol^{-1} (−41 to −54 kJ mol^{-1}) and links C have −5 to −8 kcal mol^{-1} (−21 to −33 kJ mol^{-1}).

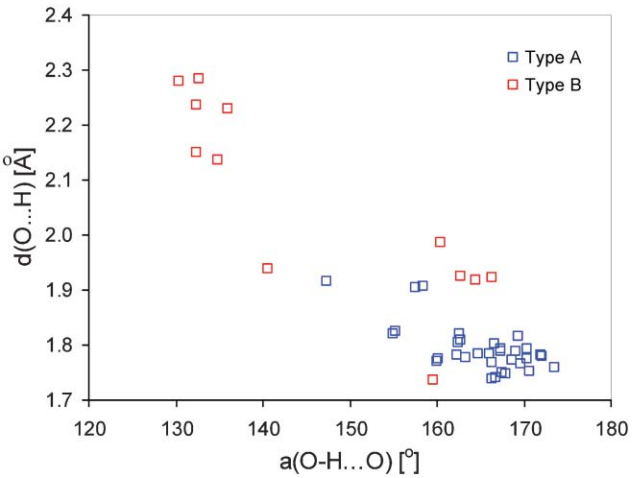

Fig. 7 The hydrogen bond distances, d(O···H), *vs.* hydrogen bond angles, a(O–H···O), for double hydrogen bonded dimers of type A (blue square) and B (red square).

3.5. Relation between melting points, chains and links

The chart in Fig. 8 shows the melting temperatures and the colours of the bars indicate the hydrogen bond motifs. Red colour is used for chains of type I or II, blue means rings or single chains and magenta means type III double chains. The red colour is dominant for the higher melting inositols whereas blue is dominant for lower melting inositols. Only myo-inositol (magenta) cannot be categorised unambiguously—despite comprising a double chain it does not have a high melting point. Thus the more complex relation of melting points to chain links has to be considered.

We now examine our four chain types, I–IV (see Fig. 4), with a view to identifying the weakest link in the chains. Fig. 9 shows the four chain types but here with the emphasis on the links. The letters A, B, and C indicate the type of dimer that forms a link in a chain, as defined in Fig. 6. Green solid lines indicate the links where a chain is likely to break when exposed to thermal energy, and blue dashed lines indicate additional hydrogen bonds not in the cooperative chain. In this context, Table 3 gives a detailed summary of the number of double/single chains per molecule and the type of the links between the

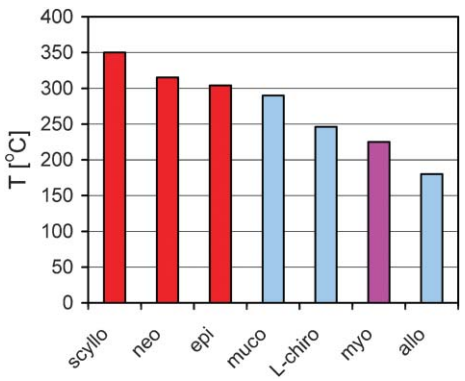

Fig. 8 Bar chart indicating the inositols in order of decreasing melting point. The colours indicate the hydrogen bond motifs: red means double chains of type I or II, blue means rings or single chains, and magenta means double chains of type IV.

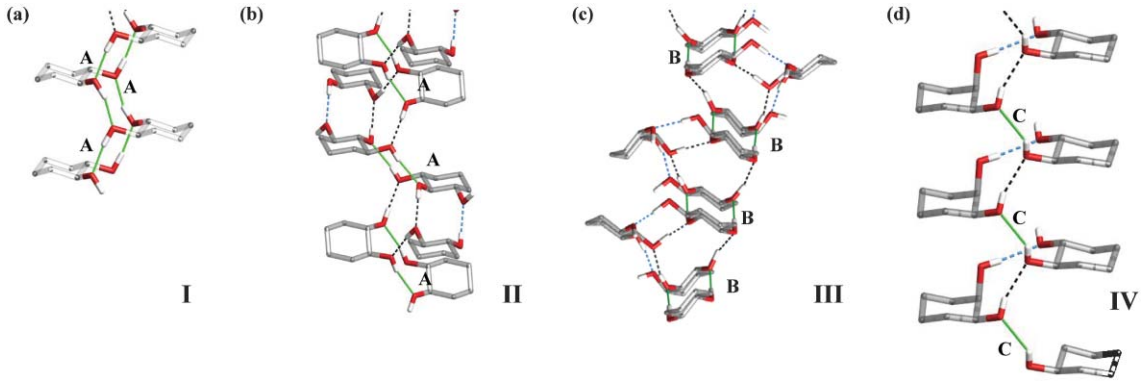

Fig. 9 Types of infinite hydrogen bond chains. (a) Type I, (b) type II, (c) type III and (d) type IV. A, B, and C indicate the types of hydrogen bonds forming links between molecules in the chain.

molecules contributing to a chain of each inositol isomer in order of decreasing melting points.

From the discussion of the different types of motifs occurring in inositol crystals (Fig. 4) it became quite clear that there is more to the stability of a stack of molecules forming an infinite chain of hydrogen bonds than purely cooperative effects. Additional hydrogen bonds linking adjacent molecules of a stack can essentially increase the stability. Regular double chains type I (Fig. 9a) have to do without this contribution; they are entirely held together by type A links, which according to our study on the molecule dimers are the strongest links occurring in inositol crystals. The only option to break these chains is to break one of the type A links, so all of them are indicated green in Fig. 9a.

The type II, antiparallel irregular double chains are strengthened in alternate links by an extra discrete hydrogen bond, which we call A*, say, and we can describe the sequence of links A, A*, A, A*, … The weakest link in these chains is A rather than A* (green highlighted link, Fig. 9b).

The type III, parallel irregular double chains (Fig. 9c) have a similarity to the type II chains just discussed. Again, we see the alternate link strengthened by an extra (discrete) hydrogen bond, and calling this link B*, we have a sequence B, B*, B, B*, … The most easily broken link is B rather than B*. We also remember that our energy calculations suggest that link B is weaker than A, so that the type III chains are more easy to disrupt than type II or I.

Type IV chains, single hydrogen bonds, have the weakest link type C. In some cases we see a strengthening of alternate links, as in epi-inositol (Fig. 8d), where we might denote the chain sequence as C, A, C, A, …, where the most easily broken link is C.

We now examine Table 3 in the light of the weakest link assigned to the chains, which join the sheets of molecules. We assume that a double link between molecules will be stronger than a single link—we are not able to say how much stronger in precise energetic terms but we know the hydrogen bond contribution dominates the energy of interaction. We used the gas phase calculation of the dimer interactions to establish that the strengths of links is in the order A > B > C. Looking at the weakest link in a chain, we see that chain types I and II really have the same weakest link A; type III has the weakest link B, which is weaker than A. Type IV has the weakest link as type C, a single hydrogen bond. Thus we estimate the robustness of the chains to breaking under thermal motion to be in the order I = II > III > IV. We see that the highest three melting points are correlated with the number of chain types I or II (scyllo-, neo- and epi-inositol). When we examine these structures having no double links, we notice that the lowest melting point (allo-inositol) has only type IV chains. Counting the number of type IV chains agrees with the observation that L-chiro-inositol has a low melting point, but higher than allo-inositol, because of the greater number of type IV chains. The melting point of myo-inositol is lower than expected if we count only the number of double linked chains, and we might expect similarity to neo-inositol, since both structures have two double chains per molecule. However, we note myo-inositol chains are type III which are weaker than types I and II.

Table 3 Melting points, number of double chains, single chains, and non-chain motifs per molecule. The type of the links within a chain/motif are types A, B and C, as shown in Fig. 6

Inositol isomer	T_m/°C	Double chains	Link	Single chain	Link	Other motif	Link	Sheets	Stacks
scyllo A	350	3 of type II	A	—	—	—	—	yes	yes
scyllo B	350	2 of type II	A	—	—	—	—	yes	yes
neo	315	2 of type I	A	—	—	—	—	yes	yes
epi	304	1 of type I	A	2 of type IV	C	—	—	yes	no
muco	290	—	—	—	—	6 ring motifs	C	yes	no
L-chiro	246	—	—	6 of type IV	C	—	—	yes	yes
myoA	225	2 type III	B	—	—	—	—	yes	yes
myo B	225	2 type III	B	—	—	—	—	yes	yes
allo	180	—	—	2 of type IV	C	4 loop motifs	C	yes	yes

The structure of muco-inositol, with a melting point above the mid-point 265 °C of the range 180–350 °C, cannot be explained by counting of double or single linked chains which are absent, and the 3-D structure is not classified as stacked sheets. However, there are extensive ring motifs consisting of twelve cooperative hydrogen bonds (Fig. 3e), which must significantly contribute to the robustness of the 3-D network.

We did not expect at the outset of this study to perfectly explain the order of the melting points using simple geometry based arguments, and we fully acknowledge the complex nature of the melting process. However, we have established an explanation of the higher (scyllo-, neo- and epi-inositol) and lower (L-chiro-, myo- and allo-inositol) melting structures based on the importance of chains of cooperative hydrogen bonds. Further quantum chemical calculations have been made on the increased stability of cooperative chains of inositols, and a forthcoming publication is intended.

In fact, the occurrence of a double chain type I or II is very rare in the CSD. Also, dimers of type A or B are not often found—this implies that most of them do not form the Type I and II chains. Seemingly, it takes a special shape of molecule to form this infinite hydrogen bond patterns—and so the inositol isomers have provided a rather special opportunity to study pairs of OH···OH···OH··· chains.

4. Conclusions

We have analysed the crystal structures of the available isomers of inositol in terms of their hydrogen bonding motifs, which we classified into chains and rings. We then paid attention to those chains and rings which show cooperative hydrogen bonding that will have increased stability compared to the sum of a set of discrete single hydrogen bonds. We identified three types of hydrogen bonded link between pairs of molecules, double-antiparallel (A), double parallel (B) and single discrete (C). We estimated the relative strengths of these links by calculating the molecular dimer interaction energy in the gas phase for A, B and C, coming to the conclusion that the strength order is A > B > C.

We classified the infinite chains of hydrogen bonds into types I, II, III and IV which link approximately planar 2-D sheets of molecules. We estimated for each chain type where the weakest link would be in the event of disruption by thermal motion, and deduced that the strength or resistance to disruption of the chains is in the order of I = II > III > IV.

We then tested our hypothesis that the presence and number of doubly linked chains of cooperative hydrogen bonds are a factor in causing higher melting points in the inositol isomers. We found that:

•The three highest melting points (scyllo-, neo- and epi-inositol) have double chains of type I or II, with *strong* type A links. Further, the number of such chains per molecule correlates with the order of melting points, scyllo- (2.5) > neo- (2) > epi-inositol (1). The isomer with the lowest melting point (allo-inositol) shows no double links, and only two type IV single bond links. L-chiro-inositol shows no double links, but six type IV links, and is also at the lower end of the melting point range.

•Muco-inositol shows no sheet structure, but extensive ring motifs comprised of single bond links type C, interlocking in a 3-D fashion, which could be consistent with its position near the mid-point of the melting point range.

•Myo-inositol has a low melting point, second to the bottom of the range, and would be anomalous if we count simply the number of double links per molecule (2), comparable with neo-inositol. However, since we found that the myo-inositol chains type III have the weaker links of type B, we can rationalise the lower melting point of myo.

Acknowledgements

The authors would like to thank Pfizer Inc. for financial support and Dr G. Day and Dr D. A. Haynes (both Pfizer Institute/Dept. of Chemistry, Cambridge, UK), Dr A. Auffret (Pfizer Global R&D, Sandwich, UK), and Dr E. Shalaev (Pfizer Global R&D, Groton, USA) for helpful discussions, and Dr M. Alfredsson (UCL, London, UK) and Prof. A. Karpfen (University of Vienna, Austria) for providing reprints of their work.

References

1 A. D. Bond, *New J. Chem.*, 2004, **28**, 104–114.
2 A. van Langevelde, R. Peschar and H. Schenk, *Chem. Mater.*, 2001, **13**, 1089–1094.
3 V. R. Thalladi, M. Nüsse and R. Boese, *J. Am. Chem. Soc.*, 2000, **122**, 9227–9236.
4 V. R. Thalladi, R. Boese and H.-C. Weiss, *Angew. Chem., Int. Ed.*, 2000, **39**, 918–922.
5 S. S. Kuduva, J. A. R. P. Sarma, A. K. Katz, H. L. Carrell and G. R. Desiraju, *J. Phys. Org. Chem.*, 2000, **13**, 719–728.
6 A. Gavezzotti, *J. Chem. Soc., Perkin Trans. 2*, 1995, 1399–1404.
7 F. E. Karasz and J. A. Pople, *J. Phys. Chem. Solids*, 1961, **20**, 294–306.
8 J. A. Pople and F. E. Karasz, *J. Phys. Chem. Solids*, 1961, **18**, 28–39.
9 A. R. Ubbelohde, *Melting and Crystal Structure*, University Press, Oxford, 1965.
10 T. Posternak, *The Cyclitols*, Hermann, Paris, 1965.
11 S. W. Watt, J. A. Chisholm, W. Jones and S. Motherwell, *J. Chem. Phys.*, 2004, **121**, 9565–9573.
12 G. A. Jeffrey, *An Introduction to Hydrogen Bonding*, Oxford University Press, Inc., New York, 1997.
13 F. A. Lindemann, *Phys. Z*, 1910, **11**, 609.
14 M. Podeschwa, O. Plettenburg, J. vom Brocke, O. Block, S. Adelt and H.-J. Altenbach, *Eur. J. Org. Chem.*, 2003, 1958–1972.
15 F. H. Allen, *Acta Crystallogr., Sect. B*, 2002, **58**, 389–397.
16 I. J. Bruno, J. C. Cole, P. R. Edgington, M. Kessler, C. F. Macrae, P. McCabe, J. Pearson and R. Taylor, *Acta Crystallogr., Sect. B*, 2002, **58**, 389–397.
17 G. M. Day, J. van de Streek, A. Bonnet, J. C. Burley, W. Jones and W. D. S. Motherwell, *Cryst. Growth Des.*, 2006, in press.
18 A. Bonnet, W. Jones and S. Motherwell, *Acta Crystallogr., Sect. E*, 2006, **62**, o2578–o2579.
19 Materials Studio 2.2, Accelrys Inc., 2002.
20 H. Sun, *J. Phys. Chem.*, 1998, **B102**, 7338–7364.
21 Cerius2 v.4.6, Accelrys Inc., San Diego, CA, 2001.
22 J. P. Perdew and Y. Wang, *Phys. Rev. B*, 1986, **33**, 8822–8824.
23 F. Sim, A. St-Amant, I. Papai and D. R. Salahub, *J. Am. Chem. Soc.*, 1992, **114**, 4391–4400.
24 C. Liang, C. S. Ewig, T. R. Stouch and A. T. Hagler, *J. Am. Chem. Soc.*, 1994, **116**, 3904–3911.
25 P. L. Polavarapu and C. S. Ewig, *J. Comput. Chem.*, 1992, **13**, 1255.
26 A. Karpfen, *Adv. Chem. Phys.*, 2002, **123**, 469–510.
27 T. Steiner, *Angew. Chem., Int. Ed.*, 2002, **41**, 48–76.
28 S. Suhai, *J. Phys. Chem.*, 1996, **100**, 3950–3958.

29 S. Suhai, *Int. J. Quantum Chem.*, 1994, **52**, 395–412.
30 A. Karpfen, A. Beyer and P. Schuster, *Int. J. Quantum Chem.*, 1981, **19**, 1113–1119.
31 M. Alfredsson, *Polar Molecules in Crystalline and Surface Environments*, PhD Thesis, Uppsala University, Uppsala, Sweden, 1999.
32 A. Bonnet, J. Chisholm, W. D. S. Motherwell and W. Jones, *CrystEngComm*, 2005, **7**, 71–75.
33 A CCDC program for visualising crystal and molecular structures, hydrogen-bonding networks, *etc*. Pluto is available for free from: The Cambridge Crystallographic Data Centre, 12 Union Road, Cambridge, CB2 1EZ, UK.
34 A. Gavezzotti and G. Filippini, *J. Phys. Chem.*, 1994, **1994**, 4831–4837.
35 G. Filippini and A. Gavezzotti, *Acta Crystallogr., Sect. B*, 1993, **49**, 868–880.

